Acta Biomaterialia 40 (2016) 235–242

Contents lists available at ScienceDirect

Acta Biomaterialia

journal homepage: www.elsevier.com/locate/actabiomat

Full length article

Surface functionalization superparamagnetic nanoparticles conjugated with thermoresponsive poly(epsilon-lysine) dendrons tethered with carboxybetaine for the mild hyperthermia-controlled delivery of VEGF ☆

S.T. Meikle [a], Y. Piñeiro [b], M. Bañobre López [c], J. Rivas [b,c], M. Santin [a,*]

[a] Brighton Studies in Tissue-mimicry and Aided Regeneration, Brighton Centre for Regenerative Medicine, University of Brighton, Brighton BN2 4GJ, UK
[b] Department of Applied Physics, University of Santiago de Compostela University, Santiago de Compostela E15782, Spain
[c] INL – International Iberian Nanotechnology Laboratory, 4715-330 Braga, Portugal

ARTICLE INFO

Article history:
Received 12 November 2015
Received in revised form 19 April 2016
Accepted 27 April 2016
Available online 28 April 2016

Keywords:
Carboxybetaine
Magnetic carriers
Mild hyperthermia
Dendrimers
VEGF

ABSTRACT

Vascular endothelial growth factor (VEGF) is the growth factor responsible for the triggering of angiogenesis, the process of blood vessel formation supporting the long-term viability of any repaired or regenerated tissue. As the growth factor is effective only when concentration gradients are generated, new shuttles need to be developed that ensure both the control of gradients at the site of tissue repair and the release of VEGF at physiological levels. Magnetic hyperthermia is the production of heat induced by magnetic materials through their exposure to an external oscillating magnetic field. In this paper, magnetic nanoparticles capable of generating controllable hyperthermia were functionalised with hyperbranched poly(epsilon-lysine) peptides integrating in their core parallel thermoresponsive elastin-like peptide sequences and presenting an uppermost branching generation tethered by the zwitterionic amino acid carboxybetaine. The results show that these functionalised magnetic nanoparticles avidly bind VEGF and release it only upon generation of mild-hyperthermic pulses generated by oscillating magnetic filed. The VEGF release occurred in a temperature range at which the elastin-like peptides collapse. It is proposed that, through the application of an external magnetic field, these magnetic carriers could generated gradients of VEGF *in vivo* and allow its tuned delivery in a number of clinical applications.

Statement of Significance

The present paper for the first time reveals the possibility to control the delivery of VEGF through mild hyperthermia stimuli generated by a oscillating magnetic field. To this purpose, magnetic nanoparticles of high size homogeneity and coated with a thin coating of poly(acrylic acid) were functionalised with a novel class of poly(epsilon lysine) dendrimers integrating in their structure a thermoresponsive amino acid sequence mimicking elastin and exposing at high density a zwitterionic modified amino acid, the carboxybetaine, known to be able to bind macromolecules. Physicochemical and biochemical characterisation elegantly show the link between the thermal properties of the nanoparticles and of the dendrimer change of conformation and how this enable the release of VEGF at temperature values compatible with the growth factor stability.

1. Introduction

Physiological angiogenesis is a key factor in any therapy aiming at the long-term viability of any regenerated of tissues [1]. Vascular endothelial growth factor (VEGF) is known to be the growth factor initiating this process and its delivery into the damaged tissue area has been proposed to stimulate the sprouting of new blood vessels from the surrounding healthy tissue [2]. As VEGF stimulates angiogenesis through very controlled concentration gradients, it is widely recognised that any therapeutic approach based on its administration need to be coupled with its spatiotemporal control [3]. It has been hypothesized that magnetic carriers of VEGF could indeed be injected into tissue with a

☆ Part of the Special Issue on Zwitterionic Materials, organized by Professors Shaoyi Jiang, Kazuhiko Ishihara, and Jian Ji.

* Corresponding author.
E-mail address: m.santin@brighton.ac.uk (M. Santin).

http://dx.doi.org/10.1016/j.actbio.2016.04.043
1742-7061/

minimally-invasive intervention and their transport across tissues could be driven by an external magnetic field capable of distributing the VEGF as a controlled gradient [4]. Indeed, the controlled transport of magnetic nanoparticles *in vivo* along a magnetic field has already been demonstrated [5]. Still, in the case of a growth factor-based therapy, the transport of VEGF in a gradient fashion need to be accompanied by its controlled delivery to the target endothelial cells. Magnetic hyperthermia is the production of heat induced by magnetic materials through their exposure to an external oscillating magnetic field. The transformation of radio-frequency (RF) magnetic energy into heat by super-paramagnetic nanoparticles (SPM-MNP) has been attributed to Néel and Brown relaxation mechanisms occurring in single-domain super-paramagnetic materials [6]. It is accepted that Néel relaxation (inner fluctuation of the magnetic moment) and Brown relaxation (rotation of the whole particle) are the magnetic loss mechanisms responsible for the heating power of SPM-MNP in a solvent and are characterised by different magnetic relaxation times, τ_N and τ_B, respectively. The efficiency of the whole set-up to transform the external magnetic energy into heat depends on both instrumental parameters (externally applied magnetic field intensity and frequency) and physico-chemical properties of the colloidally-stable nanosized systems (particle size and distribution, shape, solvent and magnetic properties of nanoparticles) [7–9]. These optimized systems have been proposed for different fields of applications including electronics, energy and biomedicine. In biomedicine, hyperthermia has mainly been used for cancer therapy through the localised generation of relatively high temperature [10–17], but its application in controlled signalling and bioactive molecule release has yet to be exploited.

Recently, colloidal suspensions of iron oxide SPM-MNPs coated with polyacrylic acid (PAA), suspended in liquids of different viscosities and concentrations, have been studied in the attempt of optimizing the conditions necessary to generate hyperthermia in biomedical applications [18]. Hyperbranched molecules such as dendrimers and dendrons, based on organic molecules, saccharides, amino acids or combinations thereof have previously been proposed for use in a number of biomedical applications [19]. Here, hyperbranched peptides based on core lysine monomers have been designed to bear a tree-like molecular structure (dendrons); (i) the root of the dendron allows the covalent grafting to poly(acrylic acid)-coated SPM-MNP iron oxide nanoparticles (Fe_3O_4@PAA), (ii) the first generation of branching is able to undergo multiple thermal transition in the range 25–42 °C and (iii) an uppermost branching generation is able to reduce MNP aggregation and facilitate the binding with bioactive molecules such as the vascular endothelial growth factor (VEGF), a growth factor playing a key role in stimulating angiogenesis, i.e. blood vessel sprouting [20]. Evidence of the thermoresponse of the grafted dendrons upon magnetic hyperthermia is provided alongside a demonstration of VEGF release in physiological buffer.

2. Materials and methods

2.1. Dendron synthesis

Poly (ε-lysine) dendrons of three (G_3K) branching generation type were synthesised on a Tenta Gel S (—NH_2) resin (Iris Biotech GmbH, Germany) using a 9-fluorenylmethoxycarbonyl (Fmoc) solid phase peptide method (Fig. 1). Dendrons were designed with a cysteine as core molecule. The resin was placed inside a reaction vessel and swollen in N,N-dimethylformamide (DMF) (Fisher Scientific UK) for 15 min. After washing with 3×7 cm^3 DMF, the addition of an acid labile Rink amide linker (Iris Biotech GmbH, Germany) to the resin was undertaken via the C-terminal of the linker. The Rink amide linker was added in a fourfold molar excess in 3 cm^3 of DMF in addition to which was added the activation agents, 0.45 M O-Benzotriazole-N,N,N′,N′-tetramethyl-uronium-hexafluoro-phosphate (HBTU) (Novabiochem, UK) and 140 μL N,N-diisopropylethylamine (DIPEA) (Sigma Aldrich Co. Ltd, UK). The coupling reaction was allowed to proceed for 30 min at room temperature. The reaction mixture was expelled from the syringe and the contents of the reaction vessel were then was then washed three times with 7 cm^3 of DMF. The base-labile Fmoc-group was removed using 20% v/v piperidine (Sigma Aldrich Co. Ltd, UK) in DMF in a series of deprotection steps at room temperature for 2 min, followed by washing with 3×7 cm^3 DMF. This procedure was repeated twice more. The exposure of N-terminal amine allowed the assembly of the established Fmoc-amino acids sequence. After the amino acid sequence were added using the coupling and deprotection steps outlined above, the peptide was allowed to stand for 30 min for a final deprotection step in 20% v/v piperidine (Sigma Aldrich Co. Ltd, UK) in DMF and washed with 3×7 cm^3 DMF. The contents of the reaction vessel were then washed with 40 cm^3 dichloromethane (Fisher Scientific, UK), methanol (Fisher Scientific, UK) and diethylether (Fisher Scientific, UK). Then, the product of synthesis was dried and weighed prior to be cleaved from the resin. Fmoc-protected groups of 50 mg dendrons were removed using two distinct mixture (i) 94% v/v trifluoroacetic acid (TFA) (Fisher Scientific, UK), 2.5% v/v deionised H_2O, 1% v/v 1–2 ethanedithiol (EDT) (Acros Organics, UK) and 2.5% v/v triisopropylsilane (TIPS) (Sigma Aldrich Co. Ltd, UK) and (ii) 88% v/v TFA, 5% v/v deionised H_2O, 5% w/v phenol (Sigma Aldrich Co. Ltd, UK) and 2% v/v TIPS at room temperature. All cleavage mixtures were prepared fresh prior to use. After three hours incubation, the solution was passed down a Pasteur pipette filled with 1 cm of a glass wool and the crude peptide was collected in a tube containing 20 cm^3 of chilled diethylether. The solution was then centrifuged (Denley BS400) at 3500 rpm for 5 min to collect the dendron. The diethylether was then carefully decanted from the tube and fresh diethylether 20 cm^3 was added and the sample was vortexed to disrupt the peptide pellet. The centrifugation procedure was then repeated twice more and the diethylether was subsequently decanted off. The reaction product was then freeze dried (Christ Alpha2-4), dissolved in ethanol and filtered through a syringe filter with a pore diameter of 0.22 μm (GE Healthcare Amersham, UK) prior to characterisation.

2.2. Dendron characterisation

Once synthesised the dendron was characterised by analytical HPLC to determine purity and further purified by further by preparative HPLC. The crude peptide was separated by a standard analytical HPLC method (Waters™ 717 plus Autosampler) performed on a hydrophobic RP 18 column (150 × 4.60 mm, Luna 3u C18 100A, Phenomenex) at 25 °C (Column chiller Model 7955, Jones Chromatography). The mobile phase consisted of a stepwise gradient of two solvent systems (Solvent A deionised water with 0.1% v/v TFA, Solvent B acetonitrile with 0.1% v/v TFA). Chromatograms were recorded on UV detector (SPO-6A, Shimadzu) and analysed by HPLC software, Total Chrom-TC Navigator. Micro-TOF mass spectrometry was used to characterise the dendron. The dendron once cleaved from the resin was dissolved in methanol (1 mg/mL) and the sample was analysed using a microTOF mass spectrometer (Bruker) with electron spray ionisation in positive ion mode. The range analysed was from 50 to 3000 m/z and fragments produced were analysed using Bruker Daltonics Data Analysis 3.4.

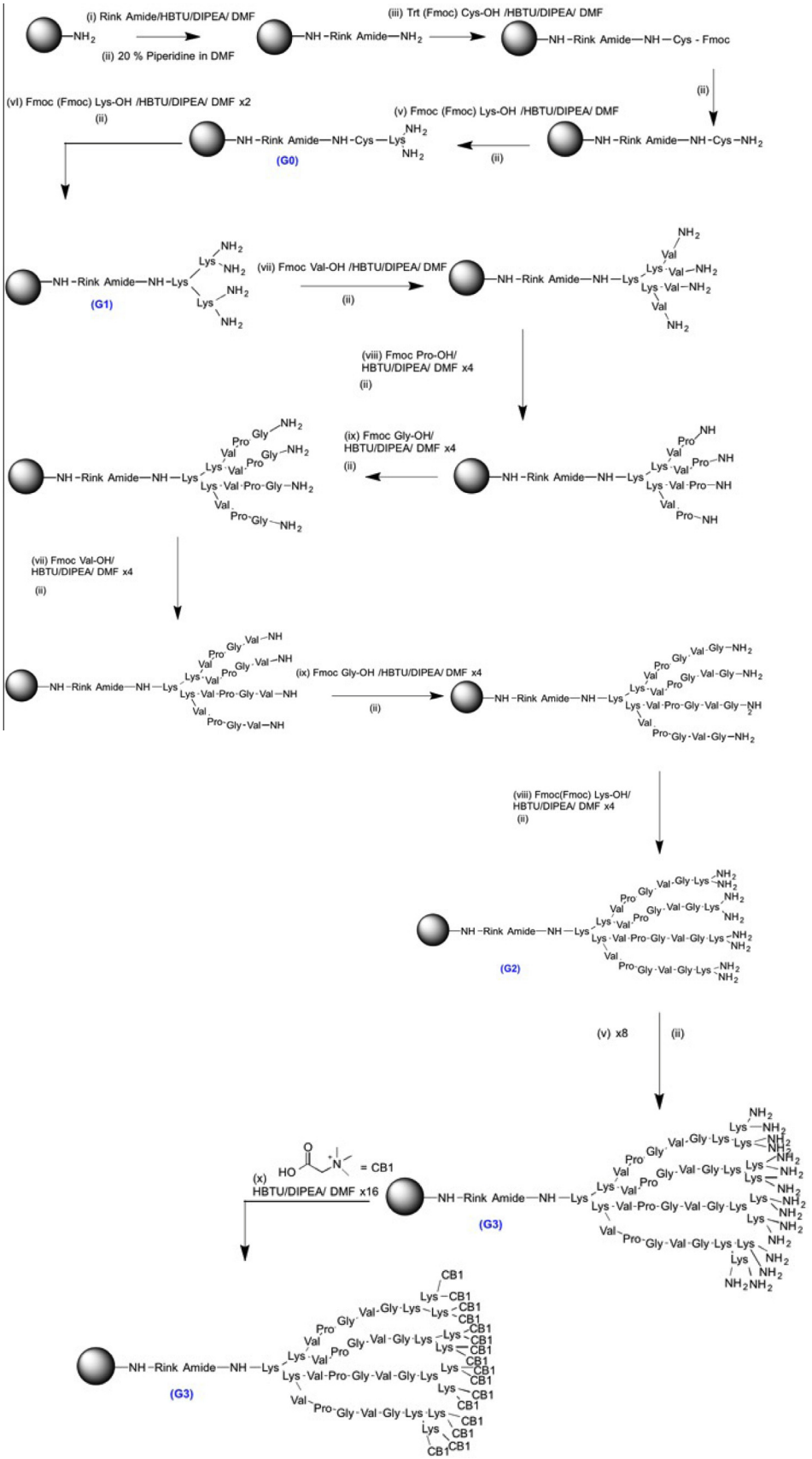

Fig. 1. Schematic representation of the solid phase synthesis of C-ELP-G_3K-Bet_{16}.

2.3. Attachment of dendron to Fe_3O_4@PAA MNP and thermal characterisation

Fe_3O_4@PAA were synthesized as previously reported [21]. Briefly, the iron oxide nanoparticles were synthesized by co-precipitation of an aqueous solution containing a stoichiometric amount of Fe^{2+} and Fe^{3+} salts with ammonium hydroxide (NH_4OH, 28%). The PAA was added in molar excess to the nanoparticle dispersion. The PAA coating has twofold effects: a) to increase the aqueous colloidal stability and b) to leave at the nanoparticle surface carboxyl functional groups susceptible of being further functionalized. As previously reported [21], the average particle size measured by transmission electron microscopy analysis resulted to be around 10 nm of diameter. XRD data (not shown) confirmed a single phase with a very good crystallinity, whereas the hysteresis loops measured in a VSM showed superparamagnetic behavior with no remanence or coercivity at zero-field and saturation magnetization as high as 60 emu/g, which is a very high value for such small NPs (data not shown).

Fe_3O_4@PAA (13 mg) were washed three times with 20 ml of ethanol. A 20 ml volume of 0.1 M MES buffer containing 38 mg EDC and 6 mg NHS was added, the solution was vortexed for 30 s and then placed in the shaking incubation for 30 min. L-cysteine (25 mg, 0.2 mmole) was added and the mixture was shaken for 1 h. The MES buffer was removed and the beads washed three times with ethanol. The beads were then split into two tubes. To conjugate the dendrimers to the cysteine via a disulfide bridge, 10 ml 8 M urea containing 3% w/v hydrogen peroxide were added along with (i) 5.3 mg, 1 μmole ELP dendrimer and (ii) 3 mg, 1 μmole of C-ELP-G_3K-Bet_{16} dendrimer. The tubes were then returned to the shaking incubator for 30 min. Scanning electron microscopy analysis was performed by a FEG-SEM Zeiss SIGMA at 5 keV on palladium-coated specimens. The SEM analysis was considered important to rule out any significant alteration of morphology and/or size of the particles after their treatment with the coupling reagents. DSC was performed twice at heating rate of 10 °C/minute, over the range −50 to 50 °C using a Mettler Toledo DSC 1 and STAR^e Thermal analysis software. Thermal transitions were studied in the 25 °C to 50 °C.

2.4. Uploading of VEGF and its release from Fe_3O_4@PAA-C-ELP-G_3K-Bet_{16}

Fe_3O_4@PAA-C-ELP-G_3K-Bet_{16} were re-suspended at 1 mg/ml in 1.25 ng to 30 μg/ml hVEGF (Abcam, UK) and incubated at 25 °C for 2 h under orbital shaking 100 rpm. The MNPs were then pelleted by centrifugation at 3500 rpm for 25 min. Excess supernatant was removed and stored for analysis by ELISA. Fe_3O_4@PAA-C-ELP-G_3K-Bet_{16} were then washed with 2 ml of ethanol and centrifuged as previously described. The supernatant was collected and analysed by ELISA. Fe_3O_4@PAA-C-ELP-G_3K-Bet_{16} were then resuspended in ethanol and added to Eppendorf tubes and allowed to air dry in a glove box at 20 °C.

Magnetic hyperthermia characterisations were performed by the means of a magnetic RF power generator operating at a frequency of f = 293 kHz and an induced magnetic field of B = 30 mT. These mild hyperthermia conditions increased significantly the temperature around the nanoparticle and induced a conformational change in the elastin moieties in a relatively short period of time to reduce any risk of significant VEGF denaturation induced by the induced temperature values that are relatively higher (up to 43 °C) than physiological body temperature. The samples were introduced in cylindrical Teflon sample holder and placed in the mid-point of an ethylene glycol cooled hollow coil (maximum of the RF magnetic field), inside a thermally isolated cylindrical Dewar glass maintained under high vacuum conditions (10^{-6} mbar). The Teflon sample holder allows the insertion of an optic–fibre thermometer tip to monitor and record the magnetic hyperthermia response (temperature increase) versus time during the application of the magnetic field.

Dried samples of Fe_3O_4@PAA-C-ELP-G_3K-Bet_{16}-VEGF were, first, dispersed in PBS by using an ultrasonic bath with a mixture of ice and water, in order to obtain a well-dispersed ferrofluid and to avoid the premature release of VEGF by ultrasound energy heating. Then, inductive heating was applied to Fe_3O_4@PAA and Fe_3O_4@-PAA-C-ELP-G_3K-Bet_{16} – VEGF ferrofluid samples with the same magnetite concentration and volume, in order to obtain a temperature increase compatible with VEGF release (above 42 °C). Accordingly to the intricate parametric dependencies of magnetic hyperthermia responses, the experimental procedure was carefully designed to optimize the magnetic heat production and to preserve the complex Fe_3O_4@PAA-C-ELP-G_3K-Bet_{16} in perfect conditions along the whole process. Therefore, from prior studies [14], the mass of Fe_3O_4@PAA-C-ELP-G_3K-Bet_{16}-VEGF sample 10 mg and volume of solvent PBS 240 μL, were chosen to obtain a ferrofluid with adequate concentration, 40 mg/mL, assuring an optimal magnetic hyperthermia response (42 °C in a few minutes) that is below the accepted denaturation point for proteins like VEGF.

During the hyperthermia experiment, VEGF charged sample was carefully monitored to avoid overheating, switching it off when the sample temperature arrived to 42 °C. Finally, the supernatant containing the released VEGF was collected after 25 min of soft centrifugation at 3500 rpm to further proceed with ELISA characterisation. Released VEGF was tested by ELISA kit (R&D Systems).

2.5. Statistical analysis

ELISA data of VEGF release were analysed by ANOVA *t* test. Data were considered significantly different at $p \leqslant 0.01$ from n = 6.

3. Results

Poly(epsilon-lysine) dendrons with three generations of branching (G_3) were obtained by solid-phase peptide synthesis. The molecular design of these dendrons included a core bi-peptide made of cysteine (Cys) and lysine (Lys) forming the root (G_0) of the molecular tree. The alpha and epsilon amino groups of the lysine were exploited to assemble additional Lys to form the first generation of branching (G_1). The linear pentapeptide (Val-Pro-Gly-Val-Gly), that is known to undergo thermal transition in the range of temperature 25–42 °C [22–26], was then assembled onto each of the four available exposed amino group. The four pentapeptide sequences were extended by the addition of a Lys monomer that allowed the branching of the macromolecule into a second generation (G_2). The third branching generation (G_3) was then assembled to expose 16 primary amine groups at the outermost terminal branches. These were finally tethered with units of carboxybetaine (Bet), a modified amino acid (i.e. trimethyl glycine), that is known to facilitate the structuring of water around its functionalities [27]. The resulting dendron [Cys-Lys-Lys_2-(Val-Pro-Gly-Val-Gly-Lys)$_4$-$(Lys)_8$-$(Bet)_{16}$] (i.e. C-ELP-G_3K-Bet_{16}) was purified by preparative HPLC (single elution peak at 14.2 min) and characterised by analytical HPLC and mass spectrometry [MS, peaks $(M + H)^{3+} = 1798$, $(M + H)^{5+} = 1079$, $(M + H)^{6+} = 896$] confirming the synthesis of the molecule at a degree of purity higher than 95% and in batches higher than 55 mg.

Purified thermoresponsive dendrons were conjugated to the PAA-SPM-MNP (Fig. 2a) that by dynamic light scattering showed a diameter of 18.46 nm, a polydispersity index of 0.331 and a zeta potential of −45.6 mV (Fig. 2b).

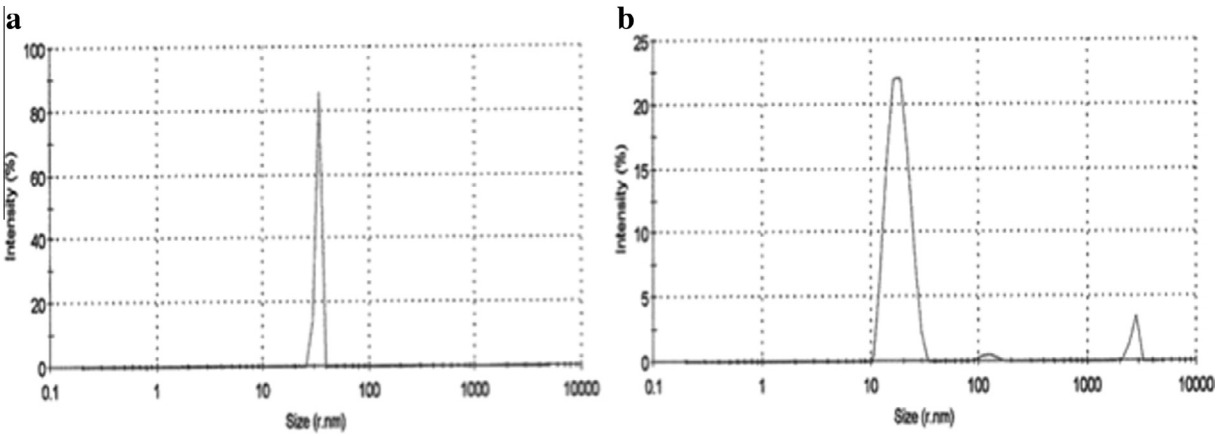

Fig. 2. Dynamic light scattering (a) Fe_3O_4@PAA-C-ELP-G_3K-Bet_{16} and (b) Fe_3O_4@PAA.

The covalent bonding of the dendron to the SMP-MNP was obtained through the formation of a disulfide bond. This was obtained by the grafting of monomers of Cys to the PAA surface of the nanoparticles the carboxylic groups of which were previously activated by mild etching in 0.1 M NaOH. The binding of the thermoresponsive dendron through its Cys root was then completed to obtain Fe_3O_4@PAA-C-ELP-G_3K-Bet_{16} of 33.37 nm in diameter, a reduced zeta potential of −25.6 mV and improved polydispersity index of 1.000 (Fig. 2a and b). Scanning electron microscopy (SEM) before and after surface functionalisation demonstrated that dendrons were able to change the topographical features of the nanoparticle surface, an electron-translucent layer always forming a contour around the nanoparticles that appeared more discrete even in the dry conditions determined by the analytical conditions (Fig. 3a and b).

The thermoresponsive properties of the unmodified and dendron-functionalised nanoparticles were studied by dynamic scanning calorimetry (DSC) and in magnetic hyperthermia conditions. DSC of the Fe_3O_4@PAA-C-ELP-G_3K-Bet_{16} was first performed in the range of temperature at which ELP peptides are known to undergo reversible transition to reach the threshold at which the irreversible molecular collapsing takes places (Fig. 4a). The DSC scan showed a first endothermic onset at 27 °C and a peak of heat absorption at 31.4 °C, which has previously been observed as the inverse temperature transition in poly pentapeptide elastin-based sequences [25]. Two additional peaks at 35.1 °C and at 43.5 °C followed. The first three thermal transitions correspond to those reported in literature for the linear ELP peptide and attributed to a constant oscillation of the molecule [22–26]. The transition occurring at the highest temperature value (43.5 °C) has being identified as the value at which the molecule undergoes irreversible collapsing caused by hydrophobic association of the ELP sequence, resulting in the expulsion of bound water molecules [26]. A second scan was then performed in the same range of

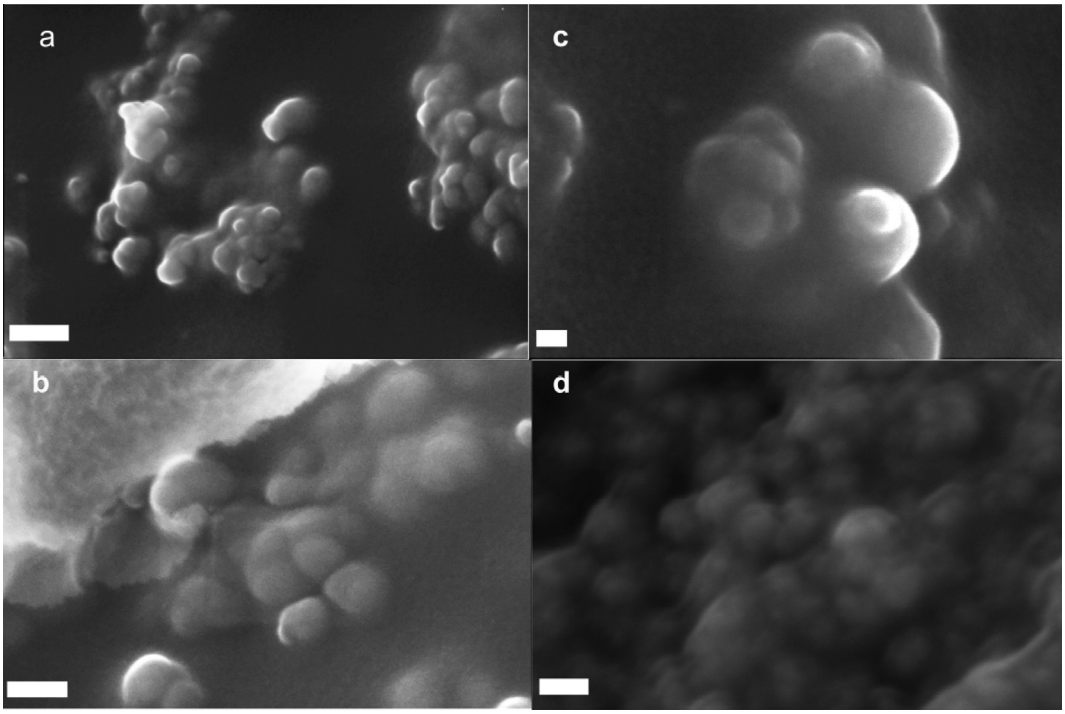

Fig. 3. Scanning electron microscopy (SEM) of Fe_3O_4@PAA (A and B) – Fe_3O_4@PAA-C-ELP-G_3K-Bet_{16}-VEGF (C and D), arrows indicate the presence of an electron translucent coating. Magnification bars in (a) and (b): 100 nm. Magnification bars in (c) and (d): 20 nm.

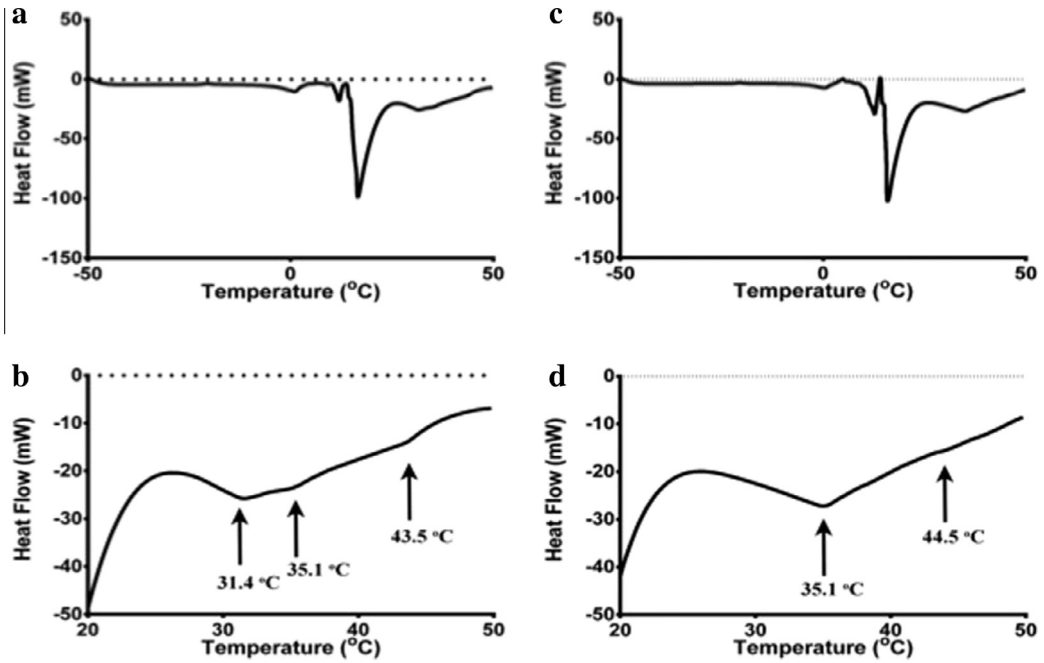

Fig. 4. Differential scanning calorimetry. First run of Fe_3O_4@PAA-C-ELP-G_3K-Bet_{16} from −50 to 50 °C at a heating rate of 10 °C/min (a). A series of transitions were observed in the range 25 to 45 °C of the first run performed (b). The sample was then cooled to −50 °C and a second run performed over the same range of temperature to confirm the irreversible collapsing of the grafted dendrons (c). Here only one major thermal transition was observed at 35 °C (d).

temperature to confirm the irreversible collapsing of the grafted dendrons (Fig. 4b). In this case, only one major thermal transition was observed at 35 °C.

These data were corroborated by the monitoring of the magnetic hyperthermia developed by Fe_3O_4@PAA and Fe_3O_4@PAA-C-ELP-G_3K-Bet_{16} when immersed in phosphate buffered saline, pH 7.4. The unmodified Fe_3O_4@PAA showed to produce a regular increase of temperature values upon exposure to the alternating current magnetic field, whereas the Fe_3O_4@PAA-C-ELP-G_3K-Bet_{16} clearly showed heat absorption at the same temperature values observed by DSC (Fig. 5, arrows). Indeed, temporary temperature plateaus were observed in the ranges 26–27 °C, 29–33 °C, 39–40 °C and 42.5 °C. Both samples reached the desired temperature increase, although large differences in the heating rate and the final temperature magnitude are observed which can be attributed to the role of the polymer coating [13]. The coating stabilizes the SPM in the solvent, not only by balancing inter-particle dipolar interactions, exchange contact interactions or electrostatic forces, but also through changes in the hydrodynamic radius that controls the Brownian relaxation time [6]. Therefore, the differences in coating width and composition for the PAA and PAA-C-ELP-G_3K-Bet_{16}-VEGF coated samples are behind their hyperthermia performance in concordance with similar ferrofluids previously reported [6].

VEGF binding on Fe_3O_4@PAA-C-ELP-G_3K-Bet_{16} was optimized to achieve a maximum loading of hVEGF of 3.64 μg/mg of Fe_3O_4@PAA-C-ELP-G_3K-Bet_{16}. The VEGF-laden magnetic shuttles were tested under the same magnetic field conditions used to study mild magnetic hyperthermia. Fig. 6 shows that no release of VEGF was observed at the middle temperature transition point that is also the body temperature and a release of 35 ng/ml corresponding approximately to 18% of the bound VEGF was achieved when hyperthermia overcame the temperature value at which the dendron undergoes molecular collapsing (43 °C). It is suggested that the loss of water molecules occurring in the dendron at this temperature threshold would lead to the collapse of the molecular structure and the consequent release of the growth factor at therapeutic concentrations. There was no complete release of the bound VEGF that may suggest the need for a more extended exposure of the carriers to the alternating magnetic field to ensure collapsing of all the dendrons. Alternatively, it could be speculated that part of the VEGF molecules have been denaturated by the thermal pulse and that the relative conformational change does not allow antibody recognition during the ELISA assay.

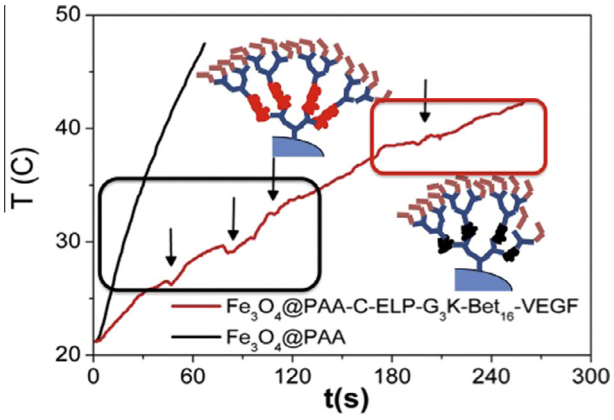

Fig. 5. Hyperthermia Treatment of Fe_3O_4@PAA and Fe_3O_4@PAA-C-ELP-G_3K-Bet_{16} samples with a volume of 240 (μL) and a magnetite concentration of 40 (g/L). These data were achieved by the monitoring of the magnetic hyperthermia developed by Fe_3O_4@PAA and Fe_3O_4@PAA-C-ELP-G_3K-Bet_{16} when immersed in phosphate buffered saline pH 7.4. The unmodified Fe_3O_4@PAA showed to produce a smooth increase of temperature values upon exposure to the alternating current magnetic field, whereas the Fe_3O_4@PAA-C-ELP-G_3K-Bet_{16} clearly showed heat absorption at the same temperature values observed by DSC (Fig. 5, arrows). Temporary temperature plateaus were observed in the ranges 26–27 °C, 29–33 °C (Black box, temperature of elastin-like peptide oscillation shown as red coil in the Fe_3O_4@PAA-C-ELP-G_3K-Bet_{16} cartoon) and 37–40 °C (Red box, temperature close to the known elastin-like peptide collapsing, black coil in the Fe_3O_4@PAA-C-ELP-G_3K-Bet_{16} cartoon). (For interpretation of the references to color in this figure legend, the reader is referred to the web version of this article.)

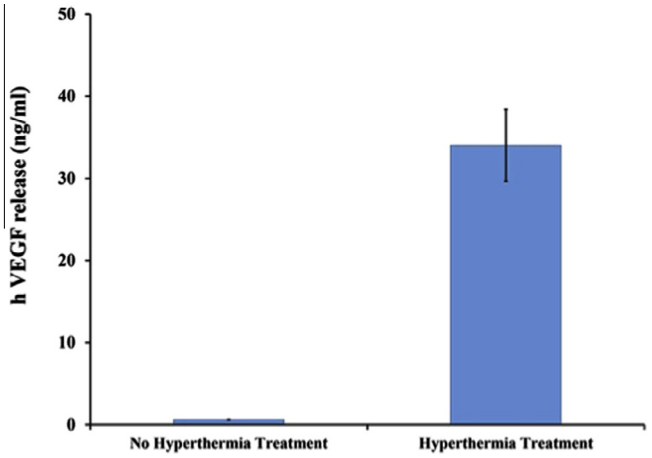

Fig. 6. Release of hVEGF from Fe_3O_4@PAA-C-ELP-G_3K-Bet_{16}-VEGF after hyperthermia treatment. Negative control shows no hVEGF release after hyperthermia treatment.

4. Discussion

The engineering of biocompatible systems able to trigger structural and conformational changes under certain physicochemical stimuli has been widely considered for therapeutic applications in regenerative medicine. In particular, nanostructures containing magnetic components are very attractive as they allow minimally-invasive, *in situ* stimulation of tissues by an external magnetic field [28]. An oscillating magnetic field can induce a temperature increase around the magnetic nanoparticle called magnetic hyperthermia. The main advantage of this thermal effect has so far demonstrated in cancer therapy where localised, high temperature heating allows the target-specific death of tumor cells and avoid the secondary cytotoxic effects derived from conventional chemotherapy treatments [28]. In this paper, a mild magnetic hyperthermia was pursued for regenerative medicine purposes rather than for the disruption of tumoral masses. The application of an external magnetic field capable of generating hyperthermia in target tissues through injected MNP carriers of bioactive molecules is a very attractive approach in any personalized treatment where different doses of the pharmaceutical substance need to be administered *in situ* on the basis of the patient's clinical conditions [28]. In addition, these magnetic nanostructures could allow a theranostic approach where the magnetic core of the carrier could provide contrast enhancement in magnetic resonance imaging of the damaged tissue during its phases of repair. More recently, biocompatible magnetic scaffolds have been reported to be able to generate magnetic field fluxes and gradients around and within their porosity through externally-applied magnetic fields [29,30]. Therefore, magnetic carriers for controlled growth factor delivery could be coupled with these scaffolds to support their rapid vascularization.

In the present paper, the proof of concept was focused on the potential of using mild magnetic hyperthermia for the controlled release of VEGF, a key growth factor in the stimulation of angiogenesis [2]. Unique to this work is the use both of super paramagnetic nanoparticles able to generate mild hyperthermia and of peptidic dendrons capable of changing conformation at those mild hyperthermia conditions. The physicochemical properties of the nanoparticles allowed the high-precision control of hyperthermia in very short ranges of time (seconds) thus avoiding any significant growth factor denaturation. The design of a class of hyperbranched peptidic dendrons able to (i) bind VEGF through the well-known properties of a zwitterionic molecule, the carboxybetaine, in preserving the bioavailability of bioactive compounds [27] and (ii) respond to the mild hyperthermia generated by the magnetic nanoparticles by the irreversible collapsing of its branched structure led to the release of the growth factor at therapeutic levels. The hyperthermia parameters fulfilled the biochemical safety recommendations for the use of magnetic hyperthermia in clinical applications that have been identified in the range of radiofrequency between several hundreds of kHz and 1 MHz within the electromagnetic spectrum. Therefore, the hyperthermia experiments have been designed to be into the safety specific absorption range (SAR) range for *in vivo* applications $H \cdot f < 4.58 \cdot 108$ ($A \cdot m^{-1} \cdot s^{-1}$) [18]. Harmful secondary effects, such as abrasions and burns, can be caused in healthy tissues outside this range [18].

Beside this main achievement, the paper has also been able to demonstrate that the functionalisation of the magnetic nanoparticles with macromolecules presenting high density carboxybetaine was also able to reduce their tendency to aggregation, a problem related to all types of nanoparticles. This was attributed to the highly hydrophilic character of carboxybetaine that is believed to form a hydration shell preventing aggregation processes [27]. Unlike previous works where the ELP peptides have shown a significant thermoresponsiveness only when integrated in polymers of relatively high molecular weight, the present work suggests that their integration in an orderly parallel structure at the first branching generation of the dendron has amplified their property to make it exploitable for the purpose of growth factor release even if part of a relatively small macromolecule.

5. Conclusions

Despite the recognised therapeutic potential of growth factors in regenerative medicine, their application in clinics is still limited by the ability of controlling their delivery in a precisely localised manner and at effective and yet safe doses. Multiple doses are also desirable to stimulate the tissue at different stages of its repair mechanism, but these are usually administrated through repeated injections causing patients distress and reduced accuracy of delivery. The magnetic nanodevice presented in this work has shown ideal properties to fulfil all the main clinical requirements for VEGF release. First of all, the reduced tendency to aggregation of the dendron-functionalised NMP, supported by the improved polydispersity index, improves their potential use in biomedical applications as it ensures the dispersion of the nanoparticles that is a pre-requisite for the optimization of the VEGF binding without the use of toxic surfactants. Moreover, these new magnetic shuttles can be delivered to the targeted tissue through the drive of a magnet to maximise their localisation at the site of regeneration and a gradient can be generated exploiting the lines and forces of the magnetic field. Once localised, the VEGF release could be controlled by pulses of mild hyperthermia to induce angiogenesis at a rate that is tuned with that of the repairing tissue.

Acknowledgement

This work was funded as part of EC project MAGISTER contract Number NMP3-LA-2008-214685.

References

[1] M.M. Martino, S. Brkic, E. Bovo, M. Burger, D.J. Schaefer, T. Wolff, L. Gürke, P.S. Briquez, H.M. Larsson, R. Gianni-Barrera, J.A. Hubbell, A. Banfi, Extracellular matrix and growth factor engineering for controlled angiogenesis in regenerative medicine, Front. Bioeng. Biotechnol. (2015), http://dx.doi.org/10.3389/fbioe.2015.00045.

[2] A. Hoeben, B. Landuyt, M.S. Highley, H. Wildiers, A.T. Van Oosterom, E.A. De Bruijn, Vascular endothelial growth factor and angiogenesis, Pharmacol. Rev. 56 (4) (2004) 549–580.

[3] Y. Brudno, A.B. Ennett-Shepard, R.R. Chen, M. Aizenberg, D.J. Mooney, Enhancing microvascular formation and vessel maturation through temporal control over multiple pro-angiogenic and pro-maturation factors, Biomaterials 34 (2013) 9201–9209.
[4] A. Banfi, G. Von Degenfeld, R. Gianni-Barrera, S. Reginato, M.J. Merchant, D.M. McDonald, H.M. Blau, Therapeutic angiogenesis due to balanced single-vector delivery of VEGF and PDGF-BB, FASEB J. 26 (2012) 2486–2497.
[5] Y. Zhang, W. Li, L. Ou, W. Wang, E. Delyagina, C. Lux, H. Sorg, K. Riehemann, G. Steinhoff, N. Ma, Targeted delivery of human VEGF gene via complexes of magnetic nanoparticle-adenoviral vectors enhanced cardiac regeneration, PLoS ONE 7 (7) (2012) e39490.
[6] R. Hergt, W. Andra, C.G. d'Ambly, I. Hilger, W.A. Kaiser, U. Richter, H.-G. Schmidt, Physical limits of hyperthermia using magnetite fine particles, IEEE Trans. Magn. 34 (1998) 3745–3754.
[7] J.P. Fortin, C. Wilhelm, J. Servais, C. Ménager, J-C Bacri, F. Gazeau, Size-sorted anionic iron oxide nanomagnets as colloidal mediators for magnetic hyperthermia, JACS 129 (2007) 2628–2635.
[8] M. Lévy, C. Wilhelm, J.-M. Siaugue, O. Horner, J.-C. Bacri, F. Gazeau, Magnetically induced hyperthermia: size-dependent heating power of γ-Fe_2O_3 nanoparticles, J. Phys.: Condens. Matter 20 (2008) 204133.
[9] M. Gonzales-Weimuller, M. Zeisberger, K.M. Krishnan, Size-dependant heating rates of iron oxide nanoparticles for magnetic fluid hyperthermia, J. Magn. Magn. Mater. 321 (2009) 1947–1950.
[10] A.S. Eggeman, S.A. Majetich, D. Farrell, Q.A. Pankhurst, Size and concentration effects on high frequency hysteresis of iron oxide nanoparticles, IEEE Trans. Magn. 43 (2007) 2451–2453.
[11] A. Jordan, R. Scholz, P. Wust, H. Fähling, R. Felix, Magnetic fluid hyperthermia (MFH): cancer treatment with AC magnetic field induced excitation of biocompatible superparamagnetic nanoparticles, J. Magn. Magn. Mater. 201 (1999) 413–419.
[12] M.W. Dewhirst, B.L. Viglianti, M. Lora-Michiels, M. Hanson, P.J. Hoopes, Basic principles of thermal dosimetry and thermal thresholds for tissue damage from hyperthermia, Int. J. Hyperthermia 19 (2003) 267–294.
[13] M. Mahmoudi, S. Sant, B. Wang, S. Laurent, T. Sen, Superparamagnetic iron oxide nanoparticles (SPIONs): development, surface modification and applications in chemotherapy, Adv. Drug Deliv. Rev. 63 (2011) 24–46.
[14] C.S.S.R. Kumar, F. Mohammad, Magnetic nanomaterials for hyperthermia-based therapy and controlled drug delivery, Adv. Drug Deliv. Rev. 63 (2011) 789–808.
[15] S.-H. Hu, B.-J. Liao, C.-S. Chiang, P.-J. Chen, S-Y. Chen, I-W. Chen, Core-shell nanocapsules stabilized by single-component polymer and nanoparticles for magneto-chemotherapy/hyperthermia with multiple drugs, Adv. Mater. 24 (2012) 3627–3632.
[16] T-J. Li, C.-C. Huang, P.-W. Ruan, K.-Y. Chuang, K.-J. Huang, D.-B. Shieh, C.-S. Yeh, *In vivo* anti-cancer efficacy of magnetite nanocrystal - based system using locoregional hyperthermia combined with 5-fluorouracil chemotherapy, Biomaterials 34 (2013) 7873–7883.
[17] J.A. Barreto, W. O'Malley, W.M. Kubeil, B. Graham, H. Stephan, L. Spiccia, Nanomaterials: applications in cancer imaging and therapy, Adv. Mater. 23 (2011) H18–H40.
[18] S. Mornet, S. Vasseur, F. Grasset, E. Duguet, Magnetic nanoparticle design for medical diagnosis and therapy, J. Mater. Chem. 14 (2004) 2161–2175.
[19] S. Svenson, D.A. Tomalia, Dendrimers in biomedical applications—reflections on the field, Adv. Drug Deliv. Rev. 57 (2005) 2106–2129.
[20] J. Street, M. Bao, L. deGuzman, S. Bunting, F.V. Peale Jr., N. Ferrara, H. Steinmetz, J. Hoeffel, J.L. Cleland, A. Daugherty, N. van Bruggen, H.P. Redmond, R.A.D. Carano, E.H. Filvaroff, Vascular endothelial growth factor stimulates bone repair by promoting angiogenesis and bone turnover, PNAS 99 (2002) 9656–9661.
[21] M. Bañobre-López, Y. Piñeiro-Redondo, M. Sandri, A. Tampieri, R. De Santis, V. A. Dediu, J. Rivas, Hyperthermia induced in magnetic scaffolds for bone tissue engineering, IEEE Trans. Magn. 50 (11) (2014) 5400507–5400514.
[22] D.W. Urry, T.L. Trapane, K.U. Prasad, Phase-structure transitions of the elastin polypentapeptide–water system within the framework of composition–temperature studies, Biopolymers 24 (1985) 2345–2356.
[23] J.C. Rodríguez-Cabello, M. Alonso, T. Pérez, M.M. Herguedas, Differential scanning calorimetry study of the hydrophobic hydration of the elastin-based polypentapeptide, poly(VPGVG), from deficiency to excess of water, Biopolymers 54 (2000) 282–288.
[24] A. Chilkoti, T. Christensen, J.A. MacKay, Stimulus responsive elastin biopolymers: applications in medicine and biotechnology, Curr. Opin. Chem. Biol. 10 (2006) 652–657.
[25] C.-H. Luan, D.W. Wry, Solvent deuteration enhancement of hydrophobicity: DSC study of the inverse temperature transition of elastin-based polypeptide, J. Phys. Chem. 95 (1991) 7896–7900.
[26] C.H. Luan, R.D. Harris, K.U. Prasad, D.W. Urry, Differential scanning calorimetry studies of the inverse transition of the polypentapeptide of elastin and its analogues, Biopolymers 29 (1990) 1699–1706.
[27] A. White, S. Jiang, Local and bulk hydration of zwitterionic glycine and its analogues through molecular simulations, J. Phys. Chem. B 115 (2011) 660–667.
[28] S.S.R.K. Challa, M. Faruq, Magnetic nanomaterials for hyperthermia-based therapy and controlled drug delivery, Adv. Drug Deliv. Rev. 63 (2011) 789–808.
[29] S.K. Samal, M. Dash, S. Shelyakova, A. Heidi, H.A. Declercq, M. Uhlarz, M. Bañobre-López, P. Dubruel, M. Cornelissen, T. Herrmannsdörfer, J. Rivas, G. Padeletti, S. De Smedt, K. Braeckmans, D.L. Kaplan, V.A. Dediu, Biomimetic magnetic silk scaffolds, ACS Appl. Mater. Interfaces 7 (11) (2015) 6282–6292.
[30] Y. Piñeiro-Redondo, M. Bañobre-López, I. Pardiñas-Blanco, G. Goya, M.A. López-Quintela, J. Rivas, The influence of colloidal parameters on the specific power absorption of PAA-coated magnetite nanoparticles, Nanoscale Res. Lett. 6 (2011) 383.